Universiteit Leiden
The Netherlands

Inflorescence lignification of natural species and horticultural hybrids of Phalaenopsis orchids

Pramanik, D.; Spaans, M.; Kranenburg, T.; Bogarin Chaves, D.G.; Heijungs, R.; Lens, F.P.; ... ; Gravendeel, B.

Inflorescence lignification of natural species and horticultural hybrids of *Phalaenopsis* orchids

Dewi Pramanik [a,b,c,*], Marlies Spaans [d], Twan Kranenburg [e], Diego Bogarin [f], Reinout Heijungs [g,h], Frederic Lens [a,b], Erik Smets [a,b,i], Barbara Gravendeel [a,b,j]

[a] *Naturalis Biodiversity Center, Darwinweg 2, Leiden 2333 CR, The Netherlands*
[b] *Intitute of Biology Leiden, Leiden University, Sylviusweg 72, Leiden 2333 BE, The Netherlands*
[c] *Indonesian Ornamental Crops Research Institute (IOCRI), Jl. Raya Ciherang, Pacet-Cianjur, West Java 43253, Indonesia*
[d] *Faculty of Science and Technology, University of Applied Sciences Leiden, Zernikedreef 11, Leiden 2333 CK, The Netherlands*
[e] *Dümmen Orange, Breeding Technology Centre, Oudecampsweg 35c, De Lier, The Netherlands*
[f] *Jardín Botánico Lankester, Universidad de Costa Rica, Cartago, Costa Rica*
[g] *Department of Operations Analytics, School of Business and Economics, Vrije Universiteit Amsterdam, De Boelelaan 1105, Amsterdam 1081 HV, The Netherlands*
[h] *Institute of Environmental Sciences (CML), Leiden University, PO Box 9518, Leiden 2300 RA, The Netherlands*
[i] *Ecology, Evolution and Biodiversity Conservation, KU Leuven, Kasteelpark Arenberg 31, P.O. Box 2435, Heverlee 3001, Belgium*
[j] *Radboud Institute for Biological and Environmental Sciences, Heyendaalseweg 135, Nijmegen 6500 GL, The Netherlands*

A B S T R A C T

Phalaenopsis is an important ornamental pot plant for the global horticultural market. The inflorescences of *Phalaenopsis* horticultural hybrids require support from a stick during plant cultivation because of the weight of multiple large flowers. Developing a horticultural hybrid with a sufficiently lignified inflorescence stem that does not require additional support could be a way to reduce the costs of production. This study aimed to (i) determine the orientation and degree of lignification in the inflorescence stem of different species and horticultural hybrids of *Phalaenopsis* and investigate whether these lignification patterns follow any (ii) topological or (iii) phylogenetic pattern of interest to further explore in genetic precision breeding. Inflorescences of comparable developmental stages of six species and 17 horticultural hybrids of flowering *Phalaenopsis* orchids were sampled. The orientation of the inflorescence varied from erect, sub-erect, arching, to pendant. The degree of lignification was measured with ImageJ using stained microscopic tissue sections and statistically analyzed. A molecular phylogeny of the species of *Phalaenopsis* was reconstructed based on plastid and nuclear ribosomal DNA sequences to analyze phylogenetic patterns. Our results show a significant difference in the degree of lignification between the different *Phalaenopsis* species and hybrids, between peduncle and rachis, and among the six different inflorescence positions analyzed. We found a positive correlation between inflorescence orientation and the proportion of lignified area per total stem area and the proportional thickness of the lignified fiber walls in the peduncle. We conclude that the degree of lignification is heritable, as we observed among our sample size a higher positive correlation between stem lignification variables among closely related taxa compared to more distantly related ones. However, a larger species sampling is needed to further validate our results.

1. Introduction

Phalaenopsis is one of the 726 orchid genera (Christenhusz and Byng, 2016). Over 73 species, seven sub-species and nine natural hybrids of *Phalaenopsis* are currently recognized (WCSP) and 37.646 horticultural hybrids are registered with the Royal Horticultural Society (RHS). *Phalaenopsis* has a major role in the world floriculture industry with a global share comprising around 10% of the international fresh-cut flower trade. The Netherlands currently has 67% of the world's orchid market share (De et al., 2015), where 8 million flowering *Phalaenopsis* plants in 2000 to 150 million in 2015 are produced (Grosscurt, 2017). This makes *Phalaenopsis* a vital export product that needs constant improvement to keep up with international competing markets (Tang and Chen, 2007). Horticultural cultivars have been produced by crossing

two or more wild species with horticultural varieties, or hybrids with hybrids (Hsu et al., 2018). The most important targets of *Phalaenopsis* breeding program include flower color, flower size, stalk length, leaf shape and ornamentation, flower longevity, ease of cultivation, and disease resistance (Hsu et al., 2018; Li et al., 2021; Tang and Chen, 2007). *Phalaenopsis* hybrids are divided into two categories: standard flowers and novelty (Tang and Chen, 2007). Cultivars in the standard flower group have few inflorescences with large-sized flowers whereas novelty group consists of new types of *Phalaenopsis* cultivars including harlequin and multifloral (Tang and Chen, 2007). The harlequin type consists of flowers with unique patterns, and is derived from *P.* 'Golden Poker', which has dramatic colors with large spots, distributed in a random pattern (Chen et al., 2004). The multiflora type has multiple inflorescences with smaller flowers (Lopez et al., 2007).

The inflorescence of *Phalaenopsis* is made up of a peduncle and a rachis: the first part is the basal one and only carries sterile bracts; the latter is the apical one and bears floral bracts and flowers that are placed distichously along the main axis. In nature, the inflorescence architecture of orchids is the compelling character for successful pollination, fruit development and seed dispersal (Iwata et al., 2012; Wyatt, 1982). Natural species and horticultural hybrids, that were developed from the natural species, have a variation of inflorescence orientations (De et al., 2015) categorized as erect, sub-erect, arching, and pendant. Many *Phalaenopsis* inflorescences have a pendant or arching orientation, which are supported by a stick during flower development in cultivation. The downside of this procedure is the amount of time and human resources it takes to replace the sticks with larger ones during plant growth, a process that cannot be robotized. A solution could be the development of hybrids that have inflorescences with an upright or erect orientation with more mechanical strength of especially the basal part so that they are not dependent on a wooden stick to stay upright.

1.1. Lignification of plants

Lignin is one of the major components of plant cell walls, and is formed by the direct deposition of polyphenolic compounds present in secondary cell walls of various cell types, notably sclerenchyma fibers and sclereids that are scattered across many different tissues and organs (Barros et al., 2015). Lignin metabolism plays a pivotal role in the adaptation to different environmental biotic and abiotic stress factors across many herbaceous and woody angiosperms (Dória et al., 2018; Dória et al., 2019; Lens et al., 2013, 2016; Schwallier et al., 2017; Thonglim et al., 2020). In orchids, lignification has been recorded from root velamen (Joca et al., 2017; Pridgeon et al., 1983), stems (Schweingruber and Börner, 2018), peduncles (Bercu et al., 2012), and fruits (Dirks-Mulder et al., 2019). In *Phalaenopsis*, lignification is reported from the stem, roots, and peduncle (Bercu et al., 2012). Research on the degree of lignification of different parts of the inflorescence of orchids in general, and *Phalaenopsis* in particular, has not yet been carried out.

1.2. Aim of this study

This study carried out an inventory of the inflorescence orientation and degree of lignification of the peduncle and rachis of a total of six natural species and 17 horticultural hybrids of *Phalaenopsis*. In addition, we also surveyed the degree of lignification of six different positions across peduncle and rachis on the basal, middle, and apical parts of four *Phalaenopsis* hybrids. The data were subsequently statistically analyzed with the aim to (i) determine the degree of lignification and (ii) investigate whether the different lignification patterns and orientation observed follow any topological and/or phylogenetic pattern to further explore in genetic precision breeding. We hypothesized the following: (1) there is a different degree of lignification between species and horticultural hybrids; (2) the most basal parts of the peduncle in general and taxa with erect peduncles in particular contain the most lignified cells;

and (3) lignification and orientation are inheritance characters for species and hybrids of *Phalaenopsis*.

2. Material and methods

2.1. Plant materials

Natural species of *Phalaenopsis* and horticultural cultivars were selected representing different orientations of the inflorescence and their economic importance (Table S1). A total of 23 different plants, consisting of six species of *Phalaenopsis* and 17 horticultural hybrids, were obtained from horticulture company Dümmen Orange, the Netherlands B.V (https://emea.dummenorange.com/site/en) and other retailers. In this research, four main types of inflorescence orientations were investigated (Fig. 1). The first category consisted of erect inflorescences, in which the peduncle and rachis have an upright position. The second category consisted of a sub-erect inflorescence, in which the peduncle and rachis have a nearly erect orientation, deviating up to 15° from a vertical orientation. The third category comprises arching inflorescences, in which the peduncle is oriented upwards but the rachis apex is facing downwards. The last category had pendant inflorescences, in which both the peduncle and rachis grow downwards. Examples of different natural species of *Phalaenopsis* with the four categories of inflorescences investigated are depicted in Fig 2.

We sampled inflorescences of comparably sized plants, of which 40–50% of the flowers were open. In this stage, the inflorescence is fully developed in *Phalaenopsis* (Christenson, 2009; Paradisoand De Pascale, 2014). In this way, we standardized sampling and ensured that tissues among the different genotypes analyzed were of a comparable developmental stage and age. The inflorescence was removed at the base of the peduncle. The freshly harvested inflorescence was dissected in two parts: the rachis (i.e., the apical part containing the flowers and floral bracts) and the peduncle (i.e., the basal part only having sterile bracts). We compared the difference in selected lignification variables in peduncle and rachis of 23 *Phalaenopsis* natural species and hybrids.

The degree of lignification was investigated in more detail at six different positions of the peduncle and rachis of four *Phalaenopsis* horticultural hybrids. These hybrids were selected based on variation in the orientation of the inflorescence of the corresponding parental lines. These were *Phalaenopsis* "Lausanne", *P.* "Liodoro", *P.* Sunny Smell and *P.* "Macassar" X "Samera", all clonally propagated.

Both the peduncle and rachis of each plant were divided into three parts: the lowest part (0.5 cm from the base of the peduncle), the middle part (0.5 cm from the second node counted from the base), and the upper part (0.5 cm from the third/last node before the onset of the rachis) of the peduncle, and the lowest part (0.5 cm from the first node of the rachis counted from the base), middle part (0.5 cm from the middle node of the rachis), and upper part of the rachis (0.5 cm from the last node of the rachis) (Fig. 3). Fresh cuttings were preserved for at least 24 h in 70% (v/v) ethanol before embedding.

2.2. LR white embedding

The LR white embedding process followed the detailed protocol described by Hamann et al. (2011). Approximately 5 mm of each transverse section of inflorescence was removed and dehydrated in ethanol absolute for at least 1 h. Next, the LR-white resin (Agar Scientific Ltd., Stansted, Essex, UK) infiltration process was initiated with increasing steps of ethanol 100%: LR White resin ratios (3:1, 2:1, 1:1, 1:2, 1:3) with an incubation time of at least 8 h for each change. The tubes were placed under vacuum with a vacuum gas pump (VWR, Radnor, Pennsylvania, USA) for 30 min between each ratio step and stored in the refrigerator during infiltration. In the last infiltration step, sections were thoroughly infiltrated in 100% LR-white resin overnight. Gelatin capsules (Electron Microscope Sciences, Hatfield, Pennsylvania, USA) were placed vertically in molds, filled with LR-white and a small
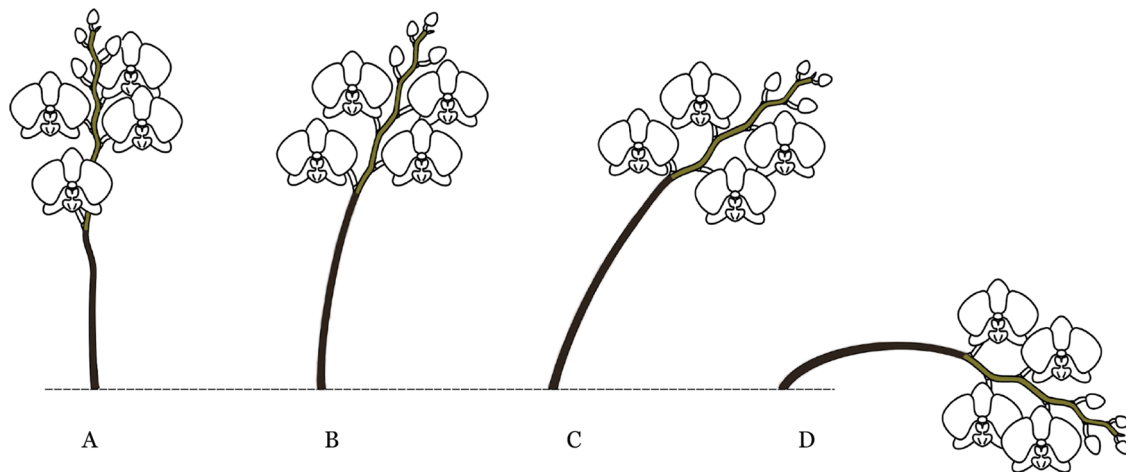
Fig. 1. Schematic overview of different orientations of the inflorescences in *Phalaenopsis*. A. Erect. B. Sub-erect. C. Arching. D. Pendant. Color code: brown= peduncle, and green= rachis. Scale bar: 1 cm. Illustrations by Esmée Winkel.

label, and stem samples were placed vertically in these molds. Finally, the closed capsules were polymerized at 60 °C for 48 h.

2.3. Sectioning and staining

Samples were sectioned using a Leica RM2265 microtome with disposable Tungsten Carbon blades (Leica, Eisenmark, Wetzlar, Germany) with a thickness of 4 μm. The sections were placed on a drop of 40% acetone on a microscope slide and fixated on a hot plate for at least 1 hr at 60 °C. The microscope slides in triplicate sections were stained with toluidine blue (1% (w/v) (VWR chemical BDH®, Radnor, Pennsylvania, USA) in 1% (w/v) borax for 30 s, then rinsed with distilled water, air-dried, and mounted with DPX new-100,579 (Merck Chemicals B.V., Amsterdam, North-Holland, the Netherlands), covered with a coverslip, and photographed after 48 h. Photographs were made with a Zeiss stacking microscope Discovery V20 (Carl Zeiss AG., Oberkochen, Germany) with Axiovision SE64 Rel. 4.9.1 software (Carl Zeiss AG., Oberkochen, Germany).

2.4. Measurement of the degree of lignification

We chose to carry out an anatomical survey and histological light microscopy to localize and quantify the lignin content of different cells (Bercu et al., 2012; Dória et al., 2018; Dória et al., 2019; Lens et al., 2013; Schwallier et al., 2017; Thonglim et al., 2020). The measurements were done with Fiji-Image J software (Schindelin et al., 2012) by using photographs of the cross-section slices made from 4 μm stained tissue sections. Light Microscope images of toluidine blue stained sections were analyzed with ImageJ (Rueden et al., 2017). Toluidine blue is used to stain polysaccharides and lignin in cell walls. The intensity of the blue color is different depending on the deposition of lignin. Higher deposition of lignin in the cells was recognized by a higher intensity (or darker) blue color of stained cell walls (Figs. 4 and 5).

Variables recorded from the sections were diameter of the stem in cross section (mm), total stem area in cross section (mm^2), and lignification characters like: lignified stem area (mm^2), proportion of lignified area per total stem area, fiber cell area (μm^2), fiber lumen area (μm^2), fiber wall area (μm^2), and proportion of fiber wall area per fiber area (which is a measurement of fiber wall thickness). We classified the degree of lignification based on the proportion of lignified area per total stem of the lowest part of the peduncle and rachis per genotype in triplicate. (Table 1 and Figs. 4 and 5).

2.5. Analysis of variance

Two different statistical analyses were performed by using a two-way MANOVA. The first analysis was carried out to determine the variation between the different natural species and horticultural hybrids on the one hand and inflorescences on the other (Data S1), and the second analysis was performed to assess the variation of the different horticultural hybrids on the one hand and the different positions on the inflorescence analyzed on the other hand (Data S2). If there were significant effects among the treatments, the mean values of the treatments were further tested using Tukey (HSD) at *p = 0.05*. The MANOVA, including the HSD-test were performed in IBM SPSS version 26 (IBM Corporate Netherlands, Amsterdam, North-Holland, the Netherlands). Data visualization of MANOVA results was made by using the ggplot2 package version 3.3.3 (Wickham, 2016) in R studio version 1.2.5033 (R Team, 2019).

2.6. Relationship between phenotypes and genotypes

Analyses were performed to investigate the correlation between dependent variables of the peduncle and rachis of the 23 *Phalaenopsis* genotypes investigated. The orientation of the inflorescence was included in this analysis with the following categories: (1) pendant: hanging downward; (2) arching: moderately curved-arched; (3) sub-erect: standing up or growing in a nearly erect position; and (4) erect: fully upright. Pearson correlation coefficients were computed using R version 3.6.2 (RC 2016) in R studio version 1.2.5033 (R Team, 2019) using the cormat package (Meyer, 2010). Pearson correlation criteria were classified as high (≥ ± 0.50 to ± 1), medium (≥ 0.30 to < ± 0.50), and low (< ± 0.30). Finally, we performed PCA analyses by operating R using the factoextra package (Kassambara and Mundt, 2020).

2.7. Genetic variation, heritability, and genetic advance of lignification characters of different species and horticultural hybrids of Phalaenopsis orchids

Lignification data from the peduncle and rachis of the 23 *Phalaenopsis* natural species and horticultural hybrids investigated were statistically analyzed as follows. The different orchid individuals were treated as 'genotypes' (expressed by variance σ^2_g) and the variety in their lignification data as 'phenotypes' (expressed by variance σ^2_p) based on Eqs. (1)–(2):

Value of phenotypic variance $\left(\sigma^2_p\right) = MSt/r$ (1)

Fig. 2. Variation of inflorescence architecture in *Phalaenopsis*. A. *Phalaenopsis pulcherrima* has an erect peduncle and rachis. B. *Phalaenopsis equestris* has an erect peduncle and sub-erect rachis. C. *Phalaenopsis amboinensis* has an arcuate peduncle and rachis. D. *Phalaenopsis amabilis* has a pendant peduncle and rachis. Photographs by Dewi Pramanik (A–C) and Suskandari Kartikaningrum (D). Scale bars: 1 cm.

Value of genotypic variance $\left(\sigma^2_g\right) = (MSt - MSe)/r$ (2)

where *MSt* is the mean square of the treatment, *MSe* is the mean square error, and *r* is the number of replications.

The genotypic coefficient of variation (*GCV*) and phenotypic coefficient of variation (*PCV*) were calculated using the following formulas, as suggested by Burton (1952).

Genotypic coefficient of variation $(GCV) = \dfrac{\sqrt{\sigma^2_g}}{x} \times 100\%$ (3)

Phenotypic coefficient of variation $(PCV) = \dfrac{\sqrt{\sigma^2_p}}{x} \times 100\%$ (4)

where *x* is the grand mean of a character. According to Deshmukh et al.

(1986), *PCV* and *GCV* values greater than 20% are regarded as high, values between 10% and 20% are regarded as a medium, and values less than 10% are considered as low.

The estimation of broad-sense heritability using the formula as suggested by Falconer (1996) was calculated as shown in Eq. (5):

Broad-sense heritability $\left(h^2_B\right) = \left(\sigma^2_g\right)/\left(\sigma^2_p\right)$ (5)

where h^2_B is broad-sense heritability. The heritability criteria were based on McWhirter (1979). Low heritability was indicated by a value of $h^2_B < 0.2$, medium heritability by $0.2 \leq h^2_B \leq 0.5$ and high heritability by $h^2_B > 0.5$.

The expected genetic advance (*GA*) and genetic advance as a percentage of the mean (*GAM*) were calculated as shown in Eq. (6) and (7):

environmental factors may affect heritability, we calculated the Genetic Advance as a percentage of the Mean (*GAM*) for predicting genetic gain in the selection process (Roychowdhury and Randrianotahina, 2011). Values of genetic advance as a percentage of the mean from 0 to 10% are recognized as low, 10 to 20% as moderate, and 20% and above as high.

2.8. Phylogenetics and ancestral state reconstruction

A molecular phylogeny of the 17 *Phalaenopsis* species assessed in this study was reconstructed based on plastid *trn*L, *trn*L-*trn*F and nuclear ribosomal *nrITS* sequences available in NCBI GenBank- (https://www.ncbi.nlm.nih.gov/genbank/) (Benson et al., 2015). We included *Hygrochilus parishii, Ornithochilus difformis,* and *Vanda tricolor* as outgroups (Zou et al., 2015). We aligned the sequences using MAFFT (Multiple Alignment using Fast Fourier Transform) and concatenated the alignments in Geneious Prime 2020 (https://www.geneious.com). Missing data were applied when a DNA sequence was not available in NCBI GenBank. These datasets were analyzed with MrBayes v.3.2.6 using the following parameters: number of generations Ngen=50 × 106 for the combined and individual datasets, number of runs (nruns=2), number of chains to run (nchains=4), temperature parameter (temp=2) and sampling frequency of 1000 yielding 50,001 trees per run. The log files from MrBayes were inspected in Tracer v.1.6 to check the convergence of independent runs (i.e. with estimated sample size (ESS) > 200). The initial 25% of trees were discarded as burn-in, and the resulting trees were used to obtain a 50% majority-rule consensus tree.

To reconstruct ancestral states (ASRs) of inflorescence architecture, we categorized peduncle and rachis orientation as either erect, sub-erect, arching, or pendant (Figs. 1 and 2). Information on inflorescence orientation was obtained from our observations and from Christenson (Christenson, 2009). Inflorescence lignification was categorized into high, medium, and low based on our measurements (Table 2). We used a randomly sampled set of 1000 trees from the post burn-in sample of the 50,000 ultrametric trees obtained from MrBayes. The ultrametric trees were obtained with PATHd8, a program for phylogenetic dating without a molecular clock (https://www2.math.su.se/PATHd8/; (Britton et al., 2007; Schoch et al., 2009).

The resulting trees and the 95% highest posterior density (HPD) estimations were visualized in FigTree v1.4.3 (Rambaut, 2006) and manipulated with R programming language (R Team, 2016) under R studio (RStudio Team, 2020) using the package APE (Paradis et al., 2004), ggtree (Yu et al., 2016), and phytools (Revell, 2012).

ASRs were analyzed with Maximum Likelihood (ML) and stochastic character mapping (SCM) using ultrametric trees (Bogarín et al., 2019). For the ML approach, we tested several models: equal rates (ER), symmetrical (SYM), and all rates different (ARD) with the re-rooting method of Yang et al. (1995) and the function ACE implemented in the R packages APE, ggtree, and phytools. A likelihood ratio test, comparing the log-likelihoods among models, was used to select the best-fitting model. Character correlations were tested with Bayesian Inference with BayesTraits V3 (Pagel, 1999, 1994; Pagel et al., 2004; Pagel and Meade, 2006). We chose the method Multistate and MCMC parameters of 30,010,000 iterations, sample period of 1000, burn-in of 10,000, auto tune rate deviation and stepping stones 100 10,000. We used the method Reversible-Jump MCMC with hyper-prior exponential to assess the best
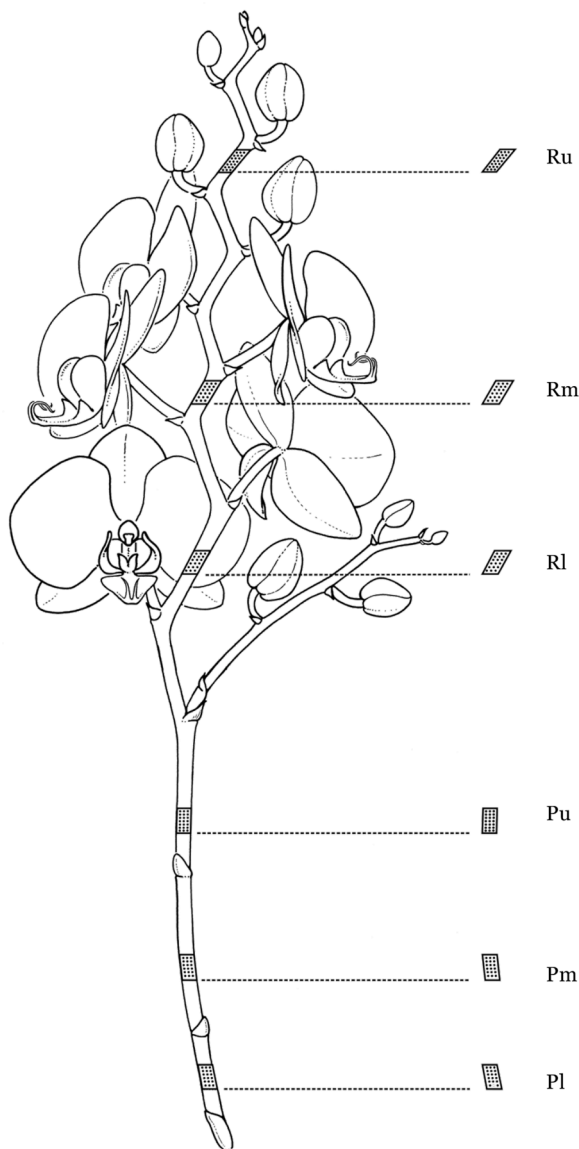
Fig. 3. Schematic overview of light microscopy sections made from six different positions distributed over the peduncle and rachis of *Phalaenopsis*. Abbreviations: Pl: lower part of peduncle, Pm: middle part of peduncle, Pu: upper part of peduncle, Rl: lower part of rachis, Rm: middle part of rachis, Ru: upper part of rachis. Scale bar: 1 cm. Illustration by Esmée Winkel.

$$GA = h^2{}_B \times \sigma_p \times k \tag{6}$$

$$GAM = (GA \, / \, x) \times 100\% \tag{7}$$

where *k* is the standardized selection differential at 5% selection intensity ($k = 2.063$), *x* is the grand mean of a character, and σ_p is the square root of phenotypic variance (Johonson et al., 1955). Since
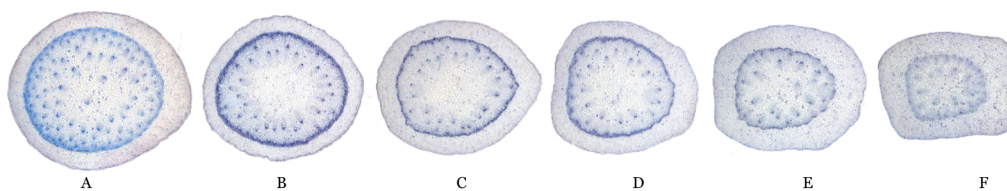
Fig. 4. Series of 4 μm thick light microscopy sections sampled from six different positions of the inflorescence of *Phalaenopsis* "Liodoro". The section was stained with toluidine blue. A lower peduncle (A), middle peduncle (B), upper peduncle (C), lower rachis (D), middle rachis (E), and upper rachis (F). Scale bar: 1 mm.
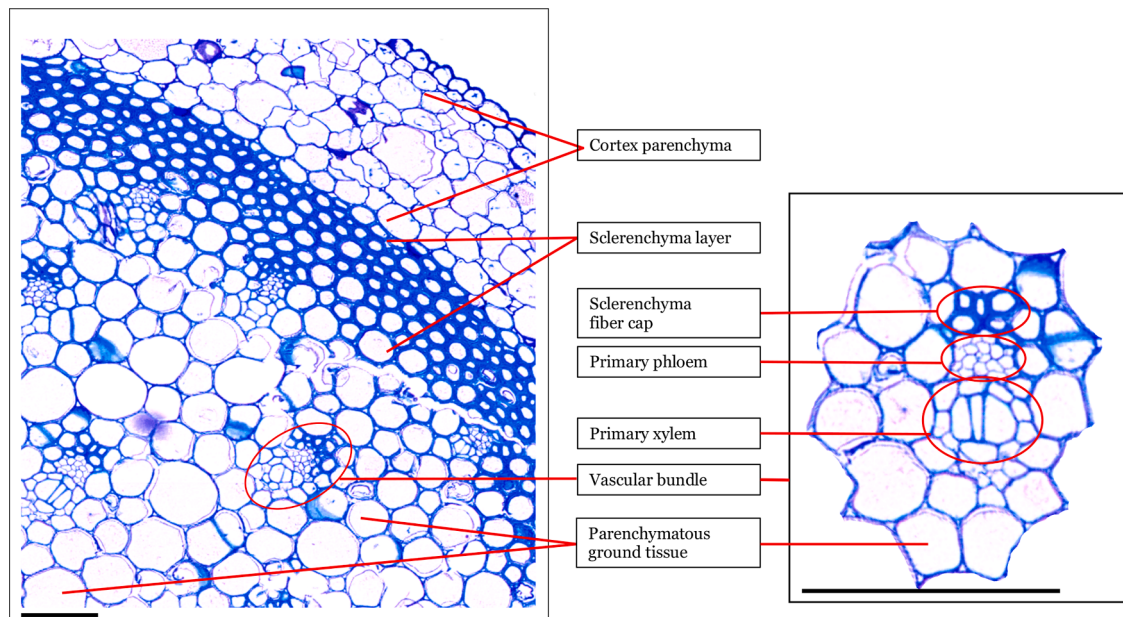
Fig. 5. Section of the lower part of the peduncle of *Phalaenopsis* "Purple Gem" stained with toluidine blue. Different tissue types are indicated. Scale bar: 100 µm.

fitting models in proportion to their posterior probabilities according to the MCMC approach. We chose the hyper-prior approach as recommended by Pagel and Meade (2006) to reduce the arbitrariness when choosing priors. We selected the option reversible jump hyper-prior exponential with prior distribution set according to the transition ranges obtained from a preliminary ML analysis. To evaluate the correlation of characters, we relied on a Bayes Factors test using the marginal likelihood from the stepping stone sampler.

3. Results

3.1. Variation in lignification of different inflorescence parts among Phalaenopsis genotypes investigated

We found a substantial variation in lignification along the peduncle and rachis across the 23 *Phalaenopsis* natural species and horticultural hybrids analyzed. The area of sclerenchyma and the area of fiber cell wall decreased from the lower part of the peduncle to the upper part of the rachis, indicating a degree of lignification corresponding to the stem development stages or the age of the tissue. The highest proportion of lignified area per total stem area (P_{LIG}) was detected in the lower part of the peduncle of *P. viridis, P.* "Purple Gem" (a horticultural hybrid resulting from crossing *P. pulcherrima* with *P. equestris*), *P.* Sunny Smell, and *P.* "Macassar" x "Samera", the lowest proportion in the rachis of *P. violacea* var. "Alba" (Data S1 and Table 2).

The stem diameter (D) of the peduncle and rachis varied between 1.61–6.12 mm. The smallest was found for the rachis of *P. amabilis* (D of 1.61 mm) and the largest for the rachis of *P.* "Liodoro" (D of 6.12 mm). The stem area (A_S) of the peduncle and rachis also varied among the genotypes and parts of the inflorescence investigated. The largest A_S was found for the peduncle of *P.* "Liodoro" (27.78 mm^2), and the smallest for the rachis of *P. amabilis* (2.16 mm^2) (Table 2).

The measurement results of characters related to lignification were as follows: the largest lignified stem area (mm^2) (A_{LIG}) was found for the peduncle of *P.* "Liodoro" (4.17 mm^2). In contrast, the smallest A_{LIG} was measured for the rachis of *P. amabilis* (0.21 mm^2). A higher proportion of lignified area per total stem area (P_{LIG}) was found for the peduncle of *P. viridis, P.* Sunny Smell, *P.* "Macassar" x "Samera", and *P.* "Purple Gem", (0.16, 0.17, 0.17, and 0.19; respectively) with the lowest found for the rachis of *P. violacea* var. "Alba" (0.06) (Table 2).

Among the genotypes tested, the largest fiber cell area (A_F) and fiber

lumen area (A_{FL}) were observed in the rachis of *P.* F4666 (1424.48 µm^2 and 1078.89 µm^2, respectively) and the smallest in the rachis *P. viridis* (321.27 µm^2, and 142,2 µm^2, respectively). The largest fiber wall area (A_{FW}) was measured for the peduncle of *P.* "Liodoro" (577.55 µm^2) and the lowest for the rachis of *P.* Sunny Smell (148.52 µm^2). The proportion of fiber wall area per fiber cell area (P_{FWA_F}) was the highest for the peduncle of *P. viridis* (0.68) and the lowest for the rachis of *P.* Sunny Smell (0.19) (Table 2).

A highly significant difference ($P = 3.43^{-115}$) in lignification characters was detected among the 23 *Phalaenopsis* genotypes. We also found a highly significant difference in the interaction between genotype and inflorescence part ($P = 9.69^{-53}$) in all variables measured (Tables S2–S5).

3.2. Detailed comparison of lignification degree of four Phalaenopsis genotypes and six inflorescence parts

To better understand the degree of lignification of different parts of the inflorescence and different *Phalaenopsis* genotypes, we analyzed six different transverse sections of the inflorescence in more detail in four different genotypes. Lignification variables were measured and calculated from sections of 4 µm thick made at these six positions. *P.* Sunny Smell had the highest percentage of lignified cell walls in the basal part of the peduncle, and the upper part of the rachis of *P.* "Lausanne" had the lowest percentage of lignified cell walls (Data S2 and Tables S6–S10). Detailed findings of each variable are described below.

The highest stem diameter (D) was observed for *P.* "Liodoro" and the smallest D was detected in *P.* "Macassar" x "Samera" (26.35 mm and 6.48 mm, respectively). There was no significant difference in D among the different positions of an inflorescence ($P = 0.41$) and among all genotypes and positions analyzed together ($P = 0.84$) (Table S9). The D only showed significant differences between the four *Phalaenopsis* genotypes investigated ($P = 2.38^{-07}$) (Table S7).

For all genotypes and positions analyzed together, the largest stem area (A_S) and the lignified stem area (mm^2) (A_{LIG}) were observed in the lowest part of the peduncle of *P.* "Liodoro" (27.78 mm^2 and 4.17 mm^2, respectively) and the smallest A_S was found in the upper part of the rachis of *P.* "Macassar" x "Samera" (3.54 mm^2), while the smallest A_{LIG} was detected in the middle and upper part of the rachis of *P.* "Macassar" x "Samera" (0.26 mm^2 and 0.24 mm^2, respectively). The highest proportion of lignified area per total stem area (P_{LIG}) was observed in the

Table 1

List of anatomical and genetic variables measured, their acronym, definitions, calculations, microscope techniques, and units.

Acronym	Definition	Calculation	Unit	Technique
D	Diameter of stem	Diameter of stem in cross section	mm	LM
A_S	Total stem area	Total stem area in cross section	mm^2	LM
A_{LIG}	Lignified stem area	Total sclerenchyma area + sclerenchyma fiber caps area in cross-section	mm^2	LM
P_{LIG}	Proportion of lignified area per total stem area	A_{LIG}/A_S	–	LM
A_F	Fiber cell area	Area of single sclerenchyma fiber cell in cross section	μm^2	LM
A_{FL}	Fiber lumen area	Area of single sclerenchyma fiber lumen in cross section	μm^2	LM
A_{FW}	Fiber wall area	$A_F - A_{FL}$ for the same fiber	μm^2	LM
$P_{FW}A_F$	Proportion of fiber wall area per fiber cell area	A_{FW}/A_F for the same fiber; a measure of sclerenchyma fiber wall thickness	–	LM
O	Inflorescence stem orientation	Scoring of the peduncle and rachis orientation: 1: pendant; 2=arcuate; 3=sub-erect;4=erect	–	Direct observation
σ^2_p	Value of phenotypic variance	Eq. (1)	–	–
σ^2_g	Value of genotypic variance	Eq. (2)	–	–
GCV	Genotypic coefficient of variation	Eq. (3)	–	–
PCV	Phenotypic coefficient of variation	Eq. (4)	–	–
h^2_B	Broad-sense heritability	Eq. (5)	–	–
GA	Genetic advance	Eq. (6)	–	–
GAM	Genetic advance as percentage of mean	Eq. (7)	–	–

basal part of the peduncle of *P.* "Macassar" x "Samera" ("(0.17) and *P.* Sunny Smell (0.17). The smallest P_{LIG} was found in the middle part of the rachis of *P.* "Macassar" x "Samera" (0.04) (Table S10).

The largest fiber cell area (A_F) and fiber lumen area (A_{FL}) were observed in the basal peduncle of *P.* Sunny Smell (1241.18 μm^2 and 921.58 μm^2, respectively). The basal peduncle of *P.* "Liodoro" has the largest fiber cell wall area (A_{FW}) (577.55 μm^2). A higher proportion of fiber wall area per fiber cell area ($P_{FW}A_F$) was obtained from the middle part of the peduncle of *P.* "Liodoro", the lower part of the peduncle and the upper part of the peduncle of *P.* "Macassar" x "Samera" (0.68, 0.67, and 0,70; respectively) (Table S10).

A highly significant difference was found between the four *Phalaenopsis* genotypes and the six positions of inflorescence, and the interaction between these factors (all $P < 0.01$ respectively). The differences among A_S, A_{LIG}, P_{LIG}, A_F, A_{FL}, A_{FW}, and $P_{FW}A_F$ were highly significant ($P < 0.01$) (Table S9).

3.3. Correlation between phenotypes and genotypes analyzed

Correlations between the characters measured were as followed: the stem diameter(D), the stem area (A_S), the lignified stem area (A_{LIG}), fiber cell area (A_F), fiber lumen area (A_{FL}), and fiber cell wall area (A_{FW}) were all significantly positively correlated for both the peduncle as well as the rachis ($r = 0.32$ to 0.97; all have $P < 0.01$). We found variations in correlation values and significance levels between the inflorescence stem orientation (O), the proportion of lignified area per total stem area (P_{LIG}), and the proportion of fiber wall area per fiber cell area ($P_{FW}A_F$) ($r = -0.82$ to 0.54) (Fig. 6).

From the peduncle and rachis, the A_{LIG} was highly positively correlated with D, A_S, A_F, and A_{FW} ($r = 0.53$ to 0.91; respectively) (all have $P < 0.01$), whereas in the rachis, A_{LIG} also had a highly positive correlation with A_{FW} ($r = 0.53$; $P < 0.01$). In the peduncle, the P_{LIG} was highly positively correlated with $P_{FW}A_F$ ($r = 0.54$; $P < 0.01$), and $P_{FW}A_F$ was negatively correlated with A_F and A_{FL} in both peduncle and rachis (peduncle: $r=-0.62$ and $r=-0.82$; rachis: $r=-0.54$ and $r= -0.69$; all have $P < 0.01$). Meanwhile, the rachis, P_{LIG} has a negative medium correlation with A_S ($r=-0.33$; $P < 0.01$). The A_{FW} of the peduncle were all significantly positively correlated with A_S, A_{LIG}, and A_F ($r = 0.60$ to 0.67; all have $P < 0.01$). As for the rachis, the A_{FW} were highly positively correlated with A_F, A_{FL}, and A_{LIG} ($r = 0.53$ to 0.73; all have $P < 0.01$). The inflorescence orientation of the peduncle has a medium positive correlation with the P_{LIG} and $P_{FW}A_F$ ($r = 0.40$ and $r = 0.31$; $P < 0.01$ and $P < 0.01$; respectively) and a medium negative correlation with A_F and A_{FL} ($r = -0.38$ and $r = -0.40$; $P < 0.01$ and $P < 0.01$; respectively). Meanwhile, for the rachis, the inflorescence orientation was negatively correlated with A_F and A_{FL} ($r = -0.31$ and $r = -0.35$; $P < 0.01$ and $P < 0.01$; respectively) (Fig. 6a and b).

To better understand the relations among the different lignification variables and genotypes investigated, we conducted a Principal Component Analysis (PCA) of the peduncle and rachis data sets. The peduncle had two PCA factors, and the rachis had three PCA factors, however, we only present the first two PCA factors in the biplot (Fig. 7): the longer the lines, the larger the loadings. In the peduncle, the first PCA was positively associated with P_{LIG}, $P_{FW}A_F$, and O (peduncle: 0.62, 0.67, and 0.64, respectively; rachis: 0.45, 0.57, 0.73, respectively). The first PCA was negatively associated with D, A_S, A_{LIG}, A_F, A_{FL}, A_{FW} (peduncle: 0.12 to 0.58; rachis: 0.02 to 0.45). In the peduncle, the second PCA was positively associated with A_F and A_{FL} (0,91 and 0.85, respectively) and negatively associated with other variables (0.26 to 0.88). Meanwhile, in the rachis, the second PCA was positively associated with A_F, A_{FL}, and P_{LIG} (0.91, 0.90, and 0.03; respectively) and negatively related to the rest of the variables (0.30 to 0.88) (Table S1) (Fig. 7 a and b).

The biplot enabled evaluating the relationships among the variables and genotypes, with the genotypes distributed near the variables being more closely correlated. The genotypes distributed at the upper part of the first PCA axis were associated with P_{LIG}, $P_{FW}A_F$, and O, indicating that these genotypes are associated with more severe lignification of peduncle and rachis. In contrast, genotypes at the lower part of the first PCA axis were negatively associated with inflorescence lignification (Tables S1 and S11) (Fig. 7a and b).

3.4. Genetic variation, heritability, and genetic advance of lignification characters of different natural species and horticultural hybrids of Phalaenopsis orchids analyzed

We detected high genetic variation, high heritability, and high genetic advance for all characters of the inflorescences of the 23 *Phalaenopsis* natural species and horticultural hybrids investigated. All characters tested had high genotypic coefficient of variation and phenotypic coefficient of variation values ($> 20\%$), a high broad-sense heritability value (> 0.9) and a high genetic advance as percentage of mean ($> 59\%$) (Table 3).

3.5. Ancestral state reconstructions

The ancestral state reconstructions of orientation and lignification of peduncle and rachis was based on the ER model. The Bayesian analysis showed that erect is the ancestral state of the orientation of peduncle

Table 2
Mean of variables measured from the interaction effects of 23 *Phalaenopsis* genotypes and two different parts of the inflorescence: the peduncle and rachis.

Genotype	Part of inflorescence	Orientation	Diameter of stem (mm)	Total stem area (mm²)	Lignified stem area (mm²)	Proportion of lignified area per total stem area	Fiber cell area (µm²)	Fiber lumen area (µm²)	Fiber wall area (µm²)	Prop0rtion of fiber wall area per fiber cell area	Classification of lignin content based on proportion of lignified area per total stem area
P.amabilis	Peduncle	Pendant	1.79 nm	2.44 rs	0.33 ut	0.14 dc	523.65 hijklm	284.45 hijklm	239.2 defghijk	0.54 abcdef	Medium
	Rachis	Pendant	1.61 n	2.16 s	0.21 u	0.1 hijklm	576.97 ghijklm	367.53 fghijklm	209.44 ghijk	0.43 efghijklm	Low
P.bastianii	Peduncle	Erect	2.92 jklmn	5.17 pqrs	0.58 opqrstu	0.11 fghi	598.04 fghijklm	352.42 fghijklm	245.61 defghijk	0.5 bcdefghij	Medium
	Rachis	Arcuate	2.74 jklmn	4.51 pqrs	0.34 stu	0.08 nopq	618.19 efghijklm	378.45 fghijklm	239.74 defghijk	0.46 cdefghijk	Low
P.javanica	Peduncle	Arcuate	3.21 ghijklmn	7.37 lmnopq	0.72 nopqrst	0.1 hijkl	705.76 defghijklm	470.37 cdefghijklm	235.38 defghijk	0.41 lmn	Low
	Rachis	Arcuate	2.80 jklmn	6.62 mnopq	0.74 mnopqrst	0.11 efgh	964.1 abcdefghi	730.75 abcdef	233.35 defghijk	0.28 lmnop	Medium
P. violacea var. "Alba"	Rachis	Pendant	2.84 jklmn	8.14 klmnop	0.47 qrstu	0.06 q	445.17 jklm	279.37 jklm	165.8 ijk	0.44 cdefghijklm	Low
P. viridis	Peduncle	Erect	3.91 cdefghijkl	9.49 jklmno	1.5 fghi	0.16 b	547.23 hijklm	202.64 klm	344.58 bcdefghij	0.68 a	High
	Rachis	Erect	2.94 jklmn	5.16 pqrs	0.54 pqrstu	0.11 ghij	321.27 m	142.42 m	178.85 hijk	0.59 abcde	Medium
P. F4373	Peduncle	Pendant	5.28 abcde	20.71 cd	2.14 bcd	0.1 ghijk	1095.45 abcde	692.22 abcdefghi	403.22 abcdef	0.44 cdefghijklm	Low
	Rachis	Pendant	4.52abcdefghijk	14.41 fghi	1.27 ghijk	0.09 ijklmno	1295.1 abc	829.17abcd	465.93 ab	0.43 efghijklm	Low
P. F3875	Peduncle	Pendant	3.69 defghijkl	10.79 ijkl	1.13 ijklmn	0.1 ghijk	1057.54 abcdefg	599.3 bcdefghijk	458.24 abc	0.47 cdefghjk	Low
	Rachis	Pendant	3.92 cdefghijkl	10.54 ijklm	1.37 ghij	0.13 cdef	1151.54 abcd	836.05 abcd	315.49 bcdefghijk	0.33 ijklmnop	Medium
P. F1405	Peduncle	Arcuate	5.07 cdefg	22.4 bc	1.96 cde	0.09 jklmno	1100.33 abcde	737.17 abcdef	363.16 bcdefgh	0.37 fghijklmno	Low
	Rachis	Pendant	4.60 abcdefghij	18.87 cde	1.43 fghij	0.08 lmnop	1108.86 abcde	823.21 abcde	285.65 bcdefghijk	0.31 klmnop	Low
P. F3380	Peduncle	Arcuate	2.68 klmn	5.84 opqrs	0.77 lmnopqrs	0.13 cde	920.32 bcdefghij	500.74 cdefghijklm	419.57 abcd	0.53 abcdefg	Medium
	Rachis	Arcuate	2.22 lmn	4.21 pqrs	0.52 pqrstu	0.12 defg	968.8 abcdefghi	599.6 bcdefghijk	369.2 bcdefgh	0.45 cdefghijkl	Medium
P. F2451	Peduncle	Arcuate	3.93 cdefghijkl	9.75 jklmno	0.74 mnopqrst	0.08 mnopq	893.07 bcdefghijk	576.64 bcdefghijkl	316.42 bcdefghijk	0.39 fghijklmn	Low
	Rachis	Arcuate	3.86 cdefghijkl	12.88 ghij	0.8 lmnopqr	0.06 pq	508.21 ijklm fghijklm	355.91 fghijklm	152.3 jk	0.33 ijklmnop	Low
P. F5124	Peduncle	Arcuate	5.51 abcd	22.29 bc	2.51 b	0.11 efgh	920.21 bcdefghij	545.23 bcdefghijklm	374.99 abcdefg	0.5 bcdefghij	Medium
	Rachis	Pendant	3.81 cdefghijkl	10.5 ijklm	0.84 klmnopq	0.08 klmnop	1101.59 abcde	832.95abcd	268.64 cdefghijk	0.31 klmnop	Low
P. F5024	Peduncle	Arcuate	5.29 abcd	21.17 cd	2.09 bcd	0.1 hijkl	1366.07 ab	925.69 ab	440.38 abc	0.38 fghijklmn	Low
	Rachis	Arcuate	3.48 efghijklmn	11.57 hijk	1.1 ijklmn	0.1 ghijk	1179.04 abced	854.24 abc	324.8 bcdefghijk	0.32 jklmnop	Low
P. F3162	Peduncle	Arcuate	4.93 abcdefghijkl	18.77 cde	1.99 cde	0.11 ijklmno	1057.74 abcdefg	694.55 abcdefgh	363.2 bcdefgh	0.39 fghijklmn	Medium
	Rachis	Pendant	3.21 ghijklmn	11.98 ijk	1 jklmno	0.08 klmnopq	1112.6 abcd	874.36 abc	238.24 defghijk	0.2 op	Low
P. F4666	Peduncle	Erect	4.66 abcdefghi	18.48 cde	2.05 cd	0.11 fghi	1089.47 abcdef	724.3 abcdef	365.18 defgh	0.37 fghijklmno	Medium
	Rachis	Sub-erect	5.57 abc	17.47 def	1.47 fghi	0.08 klmnopq	1424.48 a	1078.89 a	345.6 bcdefghi	0.27 mnop	Low

Table 2 (*continued*)

Genotype	Part of inflorescence	Orientation	Diameter of stem (mm)	Total stem area (mm²)	Lignified stem area (mm²)	Proportion of lignified area per total stem area	Fiber cell area (μm²)	Fiber lumen area (μm²)	Fiber wall area (μm²)	Prop0rtion of fiber wall area per fiber cell area	Classification of lignin content based on proportion of lignified area per total stem area
P. F4713	Peduncle	Arcuate	4.96 abcdefghi	16.5 efg	1.73 def	0.1 hijkl	924.54 bcdefghij	649.07 bcdefghi	275.46 bcdefghijk	0.34 ijklmnop	Low
	Rachis	Pendant	3.50 efghijklm	9.63 jklmno	1 jklmno	0.1 ghijk	919.64 bcdefghij	720.72 abcdefg	198.93 ghijk	0.24 nop	Low
P. F044	Peduncle	Arcuate	5.98 ab	25.62 ab	2.35 bc	0.09 ijklmno	981.24 bcdefghi	574.73 bcdefghijkl	406.5 abcde	0.47 cdefghijk	Low
	Rachis	Arcuate	4.51 abcdefghijk	15.93 efg	1.18 hijkl	0.07 opq	1158.92 abcd	819.07 abcde	339.85 bcdefghijk	0.36 ghijklmnop	Low
P. pulcherrima var. "Alba"	Peduncle	Erect	2.79 jklmn	5.26 pqrs	0.57 opqrstu	0.11 fghi	409.65 klm	227.36 jklm	182.29 ghijk	0.48 cdefghijk	Medium
	Rachis	Erect	3.08 ijklmn	5.82 opqrs	0.57 pqrstu	0.1 hijkl	519.94 hijklm	367.37 fghijklm	152.58 jk	0.35 hijklmnop	Low
P. "Liodoro"	Peduncle	Erect	5.61 abc	27.78 a	4.17 a	0.15 bc	1005.18 abcdefgh	427.63 defghijklm	577.55 a	0.62 abc	Medium
	Rachis	Erect	6.12 a	18.8 cde	1.58 efgh	0.08 lmnop	740.41 defghijklm	389.49 fghijklm	350.92 bcdefghijk	0.53 abcdefgh	Low
P. ks Super Zebra x sib	Peduncle	Erect	3.64 defghijklm	7.46 lmnopq	1.13 ijklmn	0.15 bc	728.61 defghijklm	414.81 efghijklm	313.8 bcdefghijk	0.54 abcdefg	Medium
	Rachis	Arcuate	3.94 cdefghijkl	10.3 jklmn	0.8 lmnopqr	0.08 lmnop	715.02 defghijklm	496.7 cdefghijklm	218.32 efghijk	0.37 fghijklmno	Low
P. "Purple Gem"	Peduncle	Erect	2.35 lmn	4.36 pqrs	0.85 lkmnopq	0.19 a	380.07 lm	169.51 lm	210.56 fghijk	0.62 abc	High
	Rachis	Erect	2.21 lmn	3.87 qrs	0.41 rstu	0.1 ghij	515.85 hijklm	307.06 ghijklm	208.79 ghijk	0.47 cdefghijk	Medium
P. Sunny Smell	Peduncle	Arcuate	4.90 abcdefghi	9.76 jklmno	1.62 efg	0.17 b	1241.18 abc	921.58 ab	319.6 bcdefghijk	0.31 klmnop	High
	Rachis	Arcuate	5.02 abcdefgh	10.02 jklmn	0.92 klmnop	0.09 hijklmn	999.84 abcdefghi	851.32 abc	148.52 k	0.19 p	Low
P. "Lausanne"	Peduncle	Sub-erect	4.97 abcdefgh	12.73 ghij	1.94 cde	0.15 bc	567.11 ghijklm	342.06 fghijklm	225.05 efghijk	0.44 defghijklm	Medium
	Rachis	Arcuate	4.25 abcdefghijk	10.99 ijkl	1.15 ijklm	0.1 ghij	870.94 cdefghijkl	634.86 bcdefghij	236.08 defghijk	0.33 ijklmnop	Low
P. "Macassar" x "Samera"	Peduncle	Arcuate	3.17 hijklmn	4.24 pqrs	0.72 nopqrst	0.17 b	417.97 klm	177.44 lm	240.53 defghijk	0.67 ab	High
	Rachis	Pendant	3.30 fghijklmn	6.27 nopqr	0.4 rstu	0.06 pq	445.56 jklm	288.26 hijklm	157.3 ijk	0.44 defghijklm	Low

Means followed by the same letter in the same column are not significantly different based on Tukey test, *p < 0.05*.
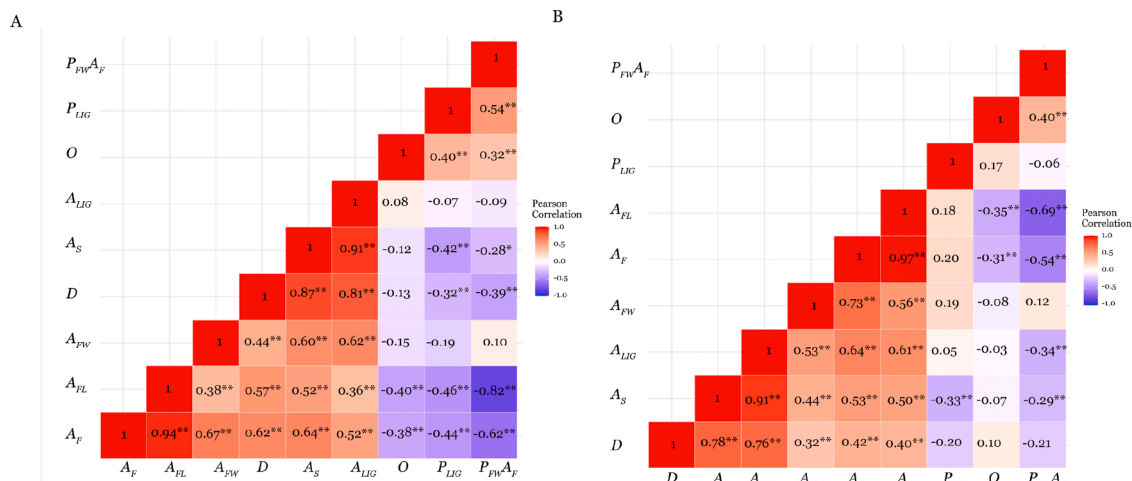
Fig. 6. Pearson correlation plot of dependent variables of the peduncle (A) and rachis (B) of the 23 *Phalaenopsis* species and horticulture hybrids analyzed in this study. ** = correlation is significant at the 0.01 level (2-tailed); * = correlation is significant at the 0.05 level (2-tailed). Person correlation color key: blue = negative correlation (below 0); white = no correlation (0); red= positive correlation (above 0). The degree of the correlation coefficients varied between high ($\geq \pm$ 0.50 to $\pm$ 1), medium ($\geq$ 0.30 to $<\pm$ 0.50) and low ($<\pm$ 0.30). Abbreviations: D= diameter of stem (mm); A_S= total stem area (mm2); A_{LIG}= lignified stem area (mm2); P_{LIG}= proportion of lignified area per total stem area; A_F = fiber cell area (µm2); A_{FL}= fiber lumen area (µm2); A_{FW} = fiber wall area (µm2); P_{FWAF} = proportion of fiber wall area per fiber cell area; and O= inflorescence stem orientation.

and rachis in *Phalaenopsis* (Fig. 9). In addition, a high lignin content of the peduncle and rachis might be the most ancestral state among the *Phalaenopsis* species sampled (Fig. 10).

4. Discussion

4.1. Lignification patterns in the inflorescences of different Phalaenopsis species and horticultural hybrids investigated

Our results indicate the degree of lignification differs among different species and horticultural *Phalaenopsis* hybrids, between cell types, cell wall layers, and stem development stages, which is in agreement with previous findings (Barros et al., 2015; Buranov and Mazza, 2008; Rencoret et al., 2008). The lignin deposition is primarily found in the concentric sclerenchyma layer in the outer stem part that surrounds the more central area, including the vascular bundles, and in the sclerenchyma fibers on top of the vascular bundles (so-called fiber caps) (Fig. 5). Lignification in the xylem of the vascular bundles is much less pronounced than that of the sclerenchyma areas.

The difference between high and low lignification degree in *Phalaenopsis* inflorescences is associated with the width of the sclerenchyma zone surrounding the central stem as well as the cell wall thickness of the fibers in this lignified area and the fiber cap area. The horticultural hybrid *P.* "Purple Gem" has the highest degree of stem lignification, leading to a higher mechanical strength of the inflorescence stems, as also have been demonstrated in many other species such as peony (Zhao et al., 2020, 2012), *Chrysanthemum* (Lv et al., 2011), sudangrass (Li et al., 2015), millet (Sreeja et al., 2016), barley (Begović et al., 2015), and rice (Li et al., 2009).

4.2. Variation in the degree of lignification of the peduncle and rachis of Phalaenopsis species and horticultural hybrids

Based on the analysis of variance, the highest proportion of lignified area per total stem area was detected in the lower part of the peduncle of *P. viridis* and *P.* "Purple Gem" (Tables 2, S2–S10). *Phalaenopsis viridis* has many flowers that open simultaneously, with thick petals and sepals. Unfortunately, this species is rarely used as a parental line and it has therefore contributed very little to the breeding of *Phalaenopsis* cultivars yet (Christenson, 2009). Our survey revealed that the inflorescence of this species has an erect orientation, a high proportion of lignified area

per total stem area, and a high fiber wall area per fiber area. These are important characters to design a breeding program for multiflora type hybrids with an erect inflorescence.

Phalaenopsis "Purple Gem" is a horticultural hybrid resulting from crossing *P. pulcherrima* with *P. equestris* (Table S1). The relatively high degree of lignification of the inflorescence of this cultivar is inherited from *P. pulcherrima.* Using *P. viridis* or *P.* "Purple Gem" as parental lines for future breeding programs may result in offspring with more lignified erect inflorescences that do not need support from sticks during inflorescence development. This is of course only the case when cross-incompatibilities, such as a different ploidy and genome size are overcome. For example, *P. pulcherrima* is estimated to have a haploid genome size of 6.16 pg while *P. amabilis*, considered to be the main founder of the standard type *Phalaenopsis* cultivars, has a haploid genome size of 1.4 pg (Lee et al., 2017). In addition, most standard flower cultivars are tetraploid while the wild *Phalaenopsis* species are diploid (Lee et al., 2020). Nevertheless, crossing between species and different cultivar groups is possible, of which *P.* "Purple Gem" is a proof.

To determine if there is a significant difference in the degree of lignification between different positions in the inflorescence of *Phalaenopsis*, the degree of lignification of six stem parts was measured in triplicate and compared. As expected, there were significant differences in the degree of lignification between the six positions (see Fig. 8). The lignified area and fiber wall area gradually decreased towards the apex of the inflorescence, as found for other monocots such as for instance *Etlingera elatior* (Zingiberaceae)(Choon and Ding, 2017). This indicates that the degree of lignification decreases in younger stem parts. Overall, lignification on top of vascular bundles (fiber caps) and the lignified zone surrounding the more central stem area including the scattered vascular bundles are key areas in the stems for maintaining peduncle strength during inflorescence development (Choon and Ding, 2017).

4.3. Correlation between lignification patterns, inflorescence architecture and ecology

The inflorescence orientation had a significant correlation with the proportion of lignified area per total stem area (P_{LIG}) and the proportion of fiber wall area per fiber cell area (P_{FWA_F}). This result indicates that the higher the degree of lignification of an inflorescence, the more erect its orientation will be. In other words, *Phalaenopsis* genotypes with a higher general degree of lignification, such as *P. viridis*, were positively
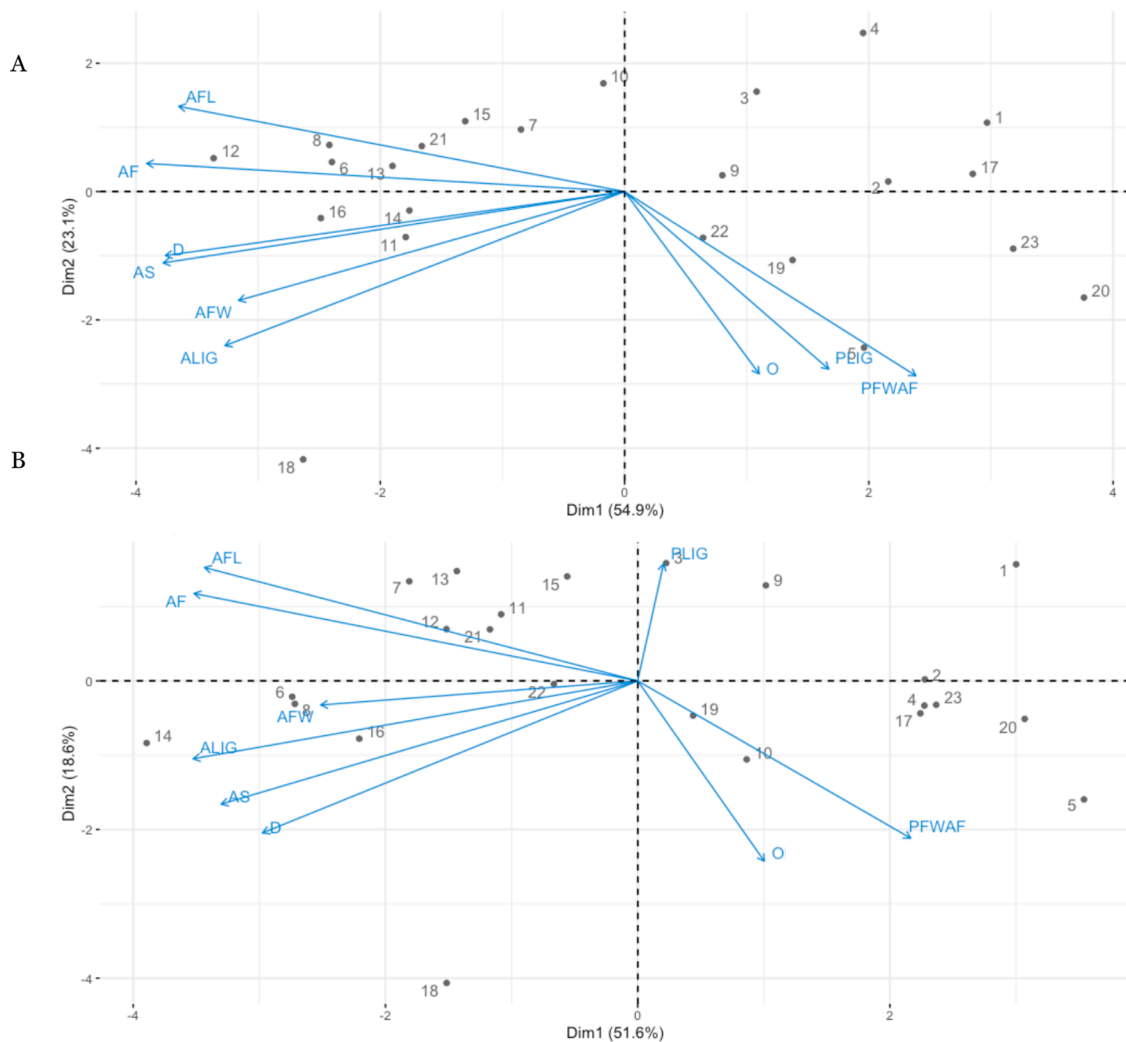
Fig. 7. Principal component analysis of lignification variables of peduncle (A) and rachis (B) of 23 *Phalaenopsis* species and horticultural hybrids. The numbers represent 23 *Phalaenopsis* species and horticultural hybrids (see Table S1). Abbreviations: D= diameter of stem (mm); A_S= total stem area (mm2); A_{LIG}= lignified stem area (mm2); P_{LIG}= proportion of lignified area per total stem area; A_F = fiber cell area (μm2); A_{FL}= fiber lumen area (μm2); AFW = fiber wall area (μm2); P_{FWAF} = proportion of fiber wall area per fiber cell area; and O= inflorescence stem orientation.

associated with the lignification characters (P_{LIG} and $P_{FW}A_F$) and orientation of inflorescence. On the contrary, genotypes with a relatively low degree of lignification, such as *P. amabilis* and *P. violacea* "Alba" were placed far from clustered lignification variables in the PCA plots. In *Arabidopsis thaliana,* gene silencing of xylem fiber lignification in inflorescence stems results in severely reduced physical properties of the stems, indicating that lignin content is essential for stem stiffness and strength (Jones et al., 2001).

From an evolutionary and ecological point of view, lignification of the inflorescence and inflorescence orientation may be strongly related to the natural habitat of a species. *P. viridis*, with erect and strongly lignified inflorescence stems, grows on limestone and in open fields (Comber, 1976). The drought and relatively low availability of nutrients in this habitat are triggers for the development of strong secondary cell wall lignification in the sclerenchyma (Barros et al., 2015). These observations confirm the previous findings in various other plant lineages that there is the link between increased stem lignification and increased drought tolerance (Dória et al., 2019; Lens et al., 2016, 2013; Thonglim et al., 2020).

Furthermore, the abundance of sunlight in open area habitat might have driven the evolution of an erect orientation of the inflorescence as plants can easily capture sunlight. In contrast, the *Phalaenopsis* species that live as epiphytes on trees under the shade of a canopy (e.g.,

P. javanica), and species that lives in swamp habitats where humidity level is high (e.g., *P. violacea*) (Christenson, 2009; Pridgeon et al., 2014), have pendant and less lignified inflorescences. In general, it has been observed that lignin deposition in stems is generally decreased under shady conditions (Hussain et al., 2019). Pendant inflorescences may have evolved in adaptation to reach and capture sufficient sunlight under a canopy. Experimental evidence for this hypothesis was obtained with the inflorescence of *A. thaliana*, where application of blue light to the inflorescence stems resulted in phototropism (Kagawa et al., 2009). Orientation of an inflorescence towards sunlight has several advantages, it might for instance optimize photosynthesis and/or attract pollinators to open flowers by generating more contrast with the background (Serrano et al., 2018).

4.4. Genetic variation, heritability, and genetic advance of different lignification traits in Phalaenopsis

The estimation of genetic parameters such as the genotypic coefficient of variation (*GCV*), phenotypic coefficient of variation (*PCV*), heritability (h^2_B) and genetic advance (*GA*) for quantitative characters is useful for conducting an effective breeding program (Amiri et al., 2018; Regmi et al., 2021; Wani et al., 2014). More specifically, *GCV* and *PCV* estimate the relative amount of variation found in the different

Table 3
Estimation of genetic parameters of characters that contribute to inflorescence lignification of 23 *Phalaenopsis* genotypes analyzed.

Characters	Genotypic variance (σ^2_g)	Phenotypic variance (σ^2_p)	Genotypic coefficient of variation (GCV) (%)	Criterion of GCV	Phenotypic coefficient of variation (PCV) (%)	Criterion of PCV	Different values between PCV and GCV	Broad- senses heritability (h^2_B)	Criterion of h^2_B	Genetic advance (GA)	Genetic advance as percentage of mean (GAM) (%)	Criterion of GAM
Inflorescence stem orientation	2.08	2.09	63.63	High	63.71	High	0.09	1.00	Broad	2.97	131.08	High
Diameter of stem (mm²)	2.14	2.24	37.71	High	38.62	High	0.91	0.95	Broad	2.95	75.98	High
Total stem area (mm²)	70.30	70.80	72.69	High	72.95	High	0.26	0.99	Broad	17.24	149.43	High
Lignified stem area (mm²)	0.70	0.71	70.10	High	70.55	High	0.45	0.99	Broad	1.72	143.70	High
Proportion of lignified area per total stem area	0.00	0.00	29.30	High	29.65	High	0.35	0.98	Broad	0.06	59.73	High
Fiber cell are (µm²)	151,862.07	159,509.92	45.92	High	47.06	High	1.14	0.95	Broad	784.43	92.43	High
Fiber lumen area (µm²)	101,277.89	106,778.75	57.13	High	58.66	High	1.53	0.95	Broad	639.40	114.78	High
Fiber wall area (µm²)	11,403.17	12,494.18	36.61	High	38.32	High	1.71	0.91	Broad	210.46	72.16	High
Proportion of fiber wall area per fiber cell area	0.02	0.02	31.96	High	32.84	High	0.88	0.95	Broad	0.27	64.18	High

characters analyzed (Roychowdhury and Randrianotahina, 2011).

The *GCV* and *PCV* values that were recorded in all characters analyzed indicates that there is a high level of variability. The difference between *PCV* and *GCV* found indicates the magnitude of the environmental effect. Small value differences between *PCV* and *GCV* were detected in all characters measured which indicates that these characters are less affected by a larger environmental effect (Saroj et al., 2021). Selection based on these characters would be most beneficial for future breeding programs to create a more lignified cultivar of *Phalaenopsis*.

According to Deshmukh et al. (1986), the *GCV* and *PCV* estimates of all characters can be categorized as high (see Table 3). A high *GCV* suggests the presence of exploitable genetic variability, which can facilitate selection (Yadav et al., 2009). On the other hand, a high *PCV* implies a high expression of both genetic and environmental effects on characters (Khan et al., 2009). The small differences in the value of *PCV* versus *GCV* suggests less influence of the environment on the expression of these characters. This means that the environmental condition does not influence the character that relates to lignification levels. The genotype with more lignified stems will benefit when its habitat changes to drier conditions. In this case, the ability of plants in regulating drought-induced embolism in the xylem is the crucial factor for a plant to survive during a period of water shortage (Thonglim et al., 2020).

Heritability is important to predict whether environmental or genetic factors influence a character. High heritability values in all characters measured indicate that genetic factors have a more significant influence than environmental factors on phenotypic appearance. Besides, broad-sense heritability also indicates whether or not there is sufficient genetic variation in a population to enable a population to respond to selection pressure (Gatti et al., 2005; Milatović et al., 2010; Ullah et al., 2012). High heritability values can be used to improve the effectiveness of selection. According to our research, the characters that directly relate to lignification such as lignified area of stem, proportion of lignified area per total stem area, fiber wall area, and proportion of fiber wall area per fiber cell area showed a high broad-sense of heritability. High genetic advance as a percentage of mean (*GAM*) was found for all characters. Heritability, together with genetic advance and *GCV*, provide the best estimations of the expected amount of advancement through phenotypic selection (Johonson et al., 1955).

4.5. Ancestral character state reconstruction of Phalaenopsis inflorescences

Based on our sampling, the character states of inflorescence orientation and lignification are phylogenetically informative in *Phalaenopsis*. Character state reconstructions show that closely related species seem to have the same orientation and degree of lignification of the inflorescence. This finding was supported by the results from the PCA analysis, showing that closely related species and horticultural hybrids had a positive correlation and association with lignification variables compared to more distantly related species, which indicates that these characters are passed on to the next generations.

The results of the Bayesian analysis showed that an erect and lignified peduncle and rachis are ancestral characters in *Phalaenopsis*. However, due to the limitations of our sample size, further analyses have to be carried out with additional genetic diversity (species and hybrids) and environmental variables to assess whether lignification characters are phylogenetically conserved throughout the entire *Phalaenopsis* genus, or whether the impact of environment is the main driver of inflorescence orientation and lignification.

5. Conclusions

The degree of lignification and inflorescence orientation are important characteristics for a breeding program for the development of *Phalaenopsis* hybrids with a rigid, upright inflorescence stem. Our surveys revealed a significant difference in lignification characters of
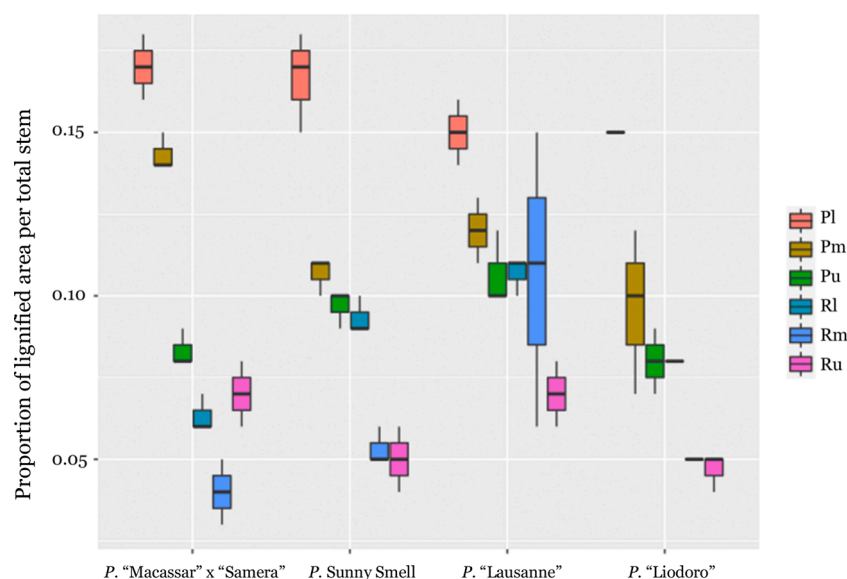
Fig. 8. Box plots of lignin content measured by calculating the proportion of lignin area per total stem area of four different *Phalaenopsis* horticultural hybrids in light microscopy sections sampled from six different positions of the inflorescence (see Fig. 3). Abbreviations: Pl=lower part of peduncle, Pm=middle part of peduncle, Pu=upper part of peduncle, Rl=lower part of rachis, Rm=middle part of rachis, Ru=upper part of rachis.
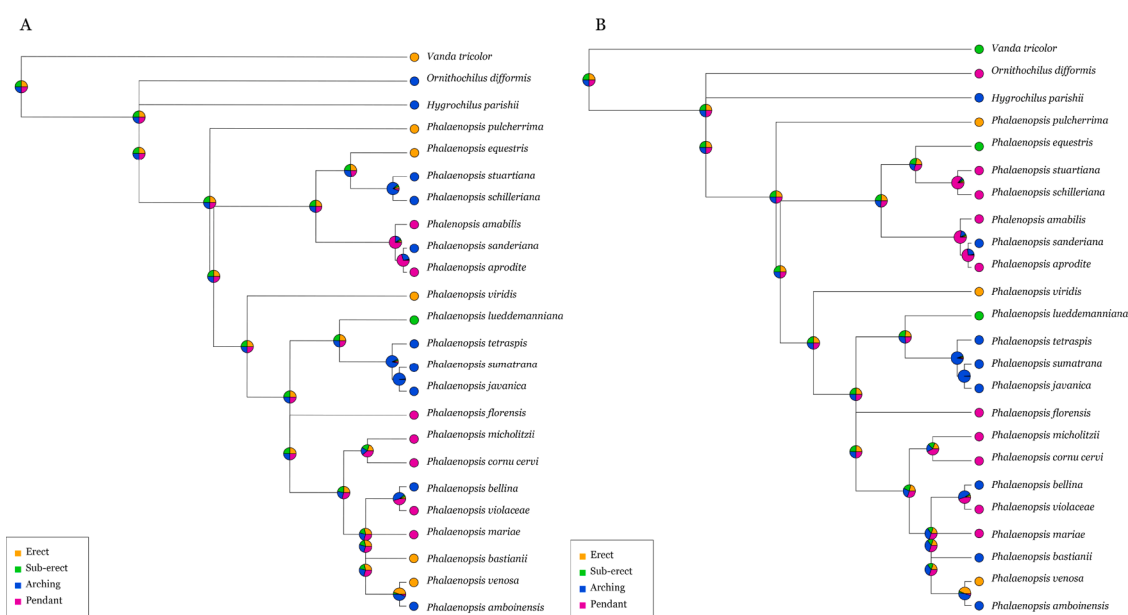

Fig. 9. Ancestral state reconstruction of orientation of the peduncle (A) and rachis (B) of 21 *Phalaenopsis* species and three outgroups from stochastic mapping analysis based on joint sampling (10,000 mapped trees). Posterior probabilities are depicted as pie charts.

inflorescences among different *Phalaenopsis* species and horticultural hybrids, between peduncle and rachis, and along six different positions on the inflorescence. Topologically the degree of lignification corresponds to the inflorescence stem developmental stages. The highest degree of lignification was found at the basal parts of the peduncle, whereas the lowest lignification was found in the apical parts of the rachis. In addition, based on our sample size, our results suggest that the degree of lignification is a heritable character as we observed a higher degree of heritability, and positive correlation between lignification variables among closely related natural species and horticultural hybrids compared to more distantly related taxa. Future work on the genes that code for lignification traits, and other molecular mechanisms underlying the spatial control of lignin deposition in *Phalaenopsis,* may help to develop a cultivar that does not need artificial support of its

inflorescences during development. Our study provides strong arguments that selection based on lignification characters contribute to such a breeding program of new *Phalaenopsis* cultivars.

CRediT authorship contribution statement

Dewi Pramanik: Conceptualization, Methodology, Formal analysis, Validation, Investigation, Writing – original draft, Writing – review & editing. **Marlies Spaans:** Formal analysis, Investigation, Validation, Writing – original draft. **Twan Kranenburg:** Conceptualization, Methodology. **Diego Bogarin:** Formal analysis. **Reinout Heijungs:** Formal analysis. **Frederic Lens:** Conceptualization, Methodology, Formal analysis, Writing – review & editing. **Erik Smets:** Conceptualization, Methodology. **Barbara Gravendeel:** Conceptualization, Validation,
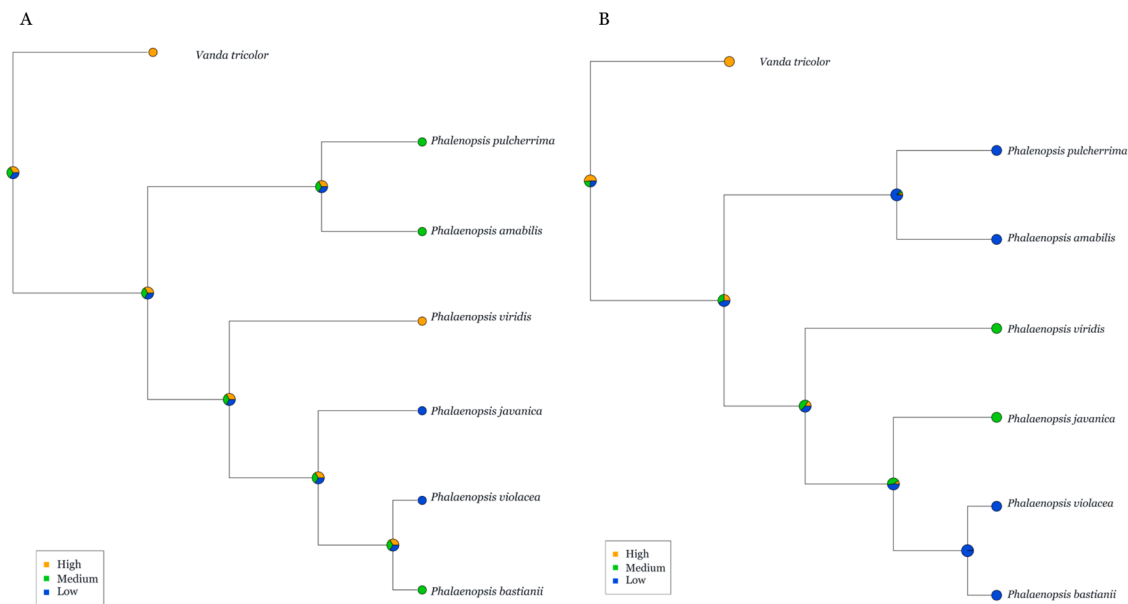
Fig. 10. Ancestral state reconstruction of the degree of lignification based on the proportion of lignified area per total stem area of peduncle (A) and rachis (B) of six *Phalaenopsis* species and one outgroup from stochastic mapping analysis based on join sampling (10,000 mapped tree). Posterior probabilities are depicted as pie charts.

Supervision, Writing – review & editing.

Declaration of Competing Interest

The authors declare that they have no known competing financial interests or personal relationships that could have appeared to influence the work reported in this paper.

Supplementary materials

Supplementary material associated with this article can be found, in the online version, at doi:10.1016/j.scienta.2021.110845.

References

Amiri, R., Bahraminejad, S., Cheghamirza, K., 2018. Estimating genetic variation and genetic parameters for grain iron, zinc and protein concentrations in bread wheat genotypes grown in Iran. J. Cereal Sci. 80, 16–23. https://doi.org/10.1016/j.jcs.2018.01.009.

Barros, J., Serk, H., Granlund, I., Pesquet, E., 2015. The cell biology of lignification in higher plants. Ann. Bot. 115, 1053–1074. https://doi.org/10.1093/aob/mcv046.

Begović, L., Ravlić, J., Lepeduš, H., Leljak-Levanić, D., Cesar, V., 2015. The pattern of lignin deposition in the cell walls of internodes during barley (Hordeum vulgare L.) Development. Acta Biol. Crac. Bot. 57, 55–66. https://doi.org/10.1515/abcsb-2015-0017.

Benson, D.A., Clark, K., Karsch-Mizrachi, I., Lipman, D.J., Ostell, J., Sayers, E.W., 2015. GenBank. Nucleic Acids Res. 43, D30–D35. https://doi.org/10.1093/nar/gku1216.

Bercu, R., Negrean, G., Broască, L., 2012. Leaf anatomical study of taxa *Salvia nemorosa* subsp. *Tesquicola, Salvia nutans* and *Salvia × dobrogensis* from Dobrudja. Acta Bot. Hung. 54, 245–257. https://doi.org/10.1556/ABot.54.2012.3-4.3.

Bogarín, D., Pérez-Escobar, O.A., Karremans, A.P., Fernández, M., Kruizinga, J., Pupulin, F., Smets, E., Gravendeel, B., 2019. Phylogenetic comparative methods improve the selection of characters for generic delimitations in a hyperdiverse Neotropical orchid clade. Sci. Rep. 9, 15098. https://doi.org/10.1038/s41598-019-51360-0.

Britton, T., Anderson, C.L., Jacquet, D., Lundqvist, S., Bremer, K., 2007. Estimating divergence times in large phylogenetic trees. Syst. Biol. 56, 741–752. https://doi.org/10.1080/10635150701613783.

Buranov, A.U., Mazza, G., 2008. Lignin in straw of herbaceous crops. Ind. Crops Prod. 28, 237–259. https://doi.org/10.1016/j.indcrop.2008.03.008.

Burton, G.W., 1952. Quantitative inheritance in grasses. In: Proceedings of 6th International Grassland Congress, pp. 277–283.

Chen, T.C., Wu, W.L., Chen, W.H., 2004. Development of harlequin flower derived from somaclone mutants of Phalaenopsis Golden Peoker "Brother. In: Proceedings of 8th Asia Pacific Orchid Conference (APOC8). Tainan, Taiwan. March 6–8, 2004Presented at the 8th Asia Pacific Orchid Conference (APOC8).

Choon, S.Y., Ding, P., 2017. Developmental changes in cellular structure and cell wall metabolism of torch ginger (*Etlingera elatior* (Jack) R.M. Smith) inflorescence. Curr. Plant Biol. 10, 3–10 [Internet.

Christenhusz, M.J.M., Byng, J.W., 2016. The number of known plants species in the world and its annual increase. Phytotaxa 261, 201. https://doi.org/10.11646/phytotaxa.261.3.1.

Christenson, E.A., 2009. Phalaenopsis: A Monograph. Timber Press.

Comber, J.B., 1976. The rediscovery of *Phalaenopsis viridis* on a limestone ridge in Indonesia. Orchid Dig. 40, 84–89.

De, L., Pathak, P., Rao, A.N., Rajeevan, P.K., 2015. Global orchid industry. In: De, L.C. (Ed.), Commercial Orchids. De Gruyter Open Poland, Warsaw, Poland, pp. 13–19.

Deshmukh, S.N., Basu, M.S., Reddy, P.S., 1986. Genetic variability, character association and path coefficients of quantitative traits in Virginia bunch varieties of groundnut. Indian J. Agric. Sci. 56, 816–821.

Dirks-Mulder, A., Ahmed, I., Broek, Uit Het, Krol, M., Menger, L., Snier, N., van Winzum, J., de Wolf, A., Van't Wout, A., Zeegers, M., Butôt, J.J., Heijungs, R., van Heuven, R., Kruizinga, B.J., Langelaan, J., Smets, R., Star, E.F., Bemer, W., Gravendeel, M., 2019. Morphological and molecular characterization of orchid fruit development. Front. Plant Sci. 10, 137. https://doi.org/10.3389/fpls.2019.00137.

Dória, Larissa Chacon, Meijs, C., Podadera, D.S., Del Arco, M., Smets, E., Delzon, S., Lens, F., 2019a. Embolism resistance in stems of herbaceous Brassicaceae and Asteraceae is linked to differences in woodiness and precipitation. Ann. Bot. 124, 1–14. https://doi.org/10.1093/aob/mcy233.

Dória, L.C., Podadera, D.S., Arco, M., Chauvin, T., Smets, E., Delzon, S., Lens, F., 2018. Insular woody daisies (*Argyranthemum,* Asteraceae) are more resistant to drought-induced hydraulic failure than their herbaceous relatives. Funct. Ecol. 32, 1467–1478. https://doi.org/10.1111/1365-2435.13085.

Falconer, D.S., 1996. Introduction to Quantitative Genetics. Longman Scientific and Technical, Harlow, UK.

Gatti, I., Anido, F.L., Vanina, C., Asprelli, P., Country, E., 2005. Heritability and expected selection response for yield traits in blanched asparagus. Genet Mol. Res. 4, 67–73.

Grosscurt, T., 2017. Becoming the Global Market Leader "The Rise of the Dutch *Phalaenopsis* Cluster. Wageningen University. Master thesis.

Hamann, T., Smets, E., Lens, F., 2011. A comparison of paraffin and resin-based techniques used in bark anatomy. Taxon 60, 841–851. https://doi.org/10.1002/tax.603016.

Hsu, C.C., Chen, H.H., Chen, W.H., 2018. Phalaenopsis. In: Van Huylenbroeck, J. (Ed.), Ornamental Crops, Handbook of Plant Breeding. Springer International Publishing, Cham, pp. 567–625. https://doi.org/10.1007/978-3-319-90698-0_23.

Hussain, S., Iqbal, N., Pang, T., Naeem Khan, M., Liu, W., Yang, W., 2019. Weak stem under shade reveals the lignin reduction behavior. J. Integr. Agric. 18, 496–505. https://doi.org/10.1016/S2095-3119(18)62111-2.

Iwata, T., Nagasaki, O., Ishii, H.S., Ushimaru, A., 2012. Inflorescence architecture affects pollinator behaviour and mating success in *Spiranthes sinensis* (Orchidaceae). New Phytol. 193, 196–203. https://doi.org/10.1111/j.1469-8137.2011.03892.x.

Joca, T.A.C., Oliveira, D.C.de, Zotz, G., Winkler, U., Moreira, A.S.F.P., 2017. The velamen of epiphytic orchids: variation in structure and correlations with nutrient absorption. Flora 230, 66–74. https://doi.org/10.1016/j.flora.2017.03.009.

Johonson, H., Robinson, H., Comostock, R., 1955. Genotypic and phenotypic correlations in soybeans and their implication in selection. Agron. J. 47, 477–483.

Jones, L., Ennos, A.R., Turner, S.R., 2001. Cloning and characterization of irregular xylem4 (irx4): a severely lignin-deficient mutant of Arabidopsis. Plant J. 26, 205–216. https://doi.org/10.1046/j.1365-313x.2001.01021.x.

Kagawa, T., Kimura, M., Wada, M., 2009. Blue light-induced phototropism of inflorescence stems and petioles is mediated by phototropin family members phot1 and phot2. Plant Cell Physiol. 50, 1774–1785. https://doi.org/10.1093/pcp/pcp119.

Kassambara, A., Mundt, F., 2020. factoextra: extract and visualize the results of multivariate data analyses. CRAN.R-project.org.

Khan, A., Kabir, M.Y., Alam, M.M., 2009. Variability, correlation path analysis of yield and yield components of pointed gourd. J. Agric. Rural Dev. 93–98.

Lee, Y.I., Chung, M.C., Kuo, H.C., Wang, C.N., Lee, Y., Lin, C.Y., Jiang, H., Yeh, C.H., 2017. The evolution of genome size and distinct distribution patterns of rDNA in *Phalaenopsis* (Orchidaceae). Botan. J. Linn. Soc. 185, 65–80. https://doi.org/10.1093/botlinnean/box049.

Lee, Y.I., Tseng, Y., Lee, Y.C., Chung, M.C., 2020. Chromosome constitution and nuclear DNA content of *Phalaenopsis* hybrids. Sci. Hortic. (Amsterdam) 262, 109089. https://doi.org/10.1016/j.scienta.2019.109089.

Lens, F., Picon-Cochard, C., Delmas, C.E.L., Signarbieux, C., Buttler, A., Cochard, H., Jansen, S., Chauvin, T., Doria, L.C., Del Arco, M., Delzon, S., 2016. Herbaceous angiosperms are not more vulnerable to drought-induced embolism than angiosperm trees. Plant Physiol 172, 661–667. https://doi.org/10.1104/pp.16.00829.

Lens, F., Tixier, A., Cochard, H., Sperry, J.S., Jansen, S., Herbette, S., 2013. Embolism resistance as a key mechanism to understand adaptive plant strategies. Curr. Opin. Plant Biol. 16, 287–292. https://doi.org/10.1016/j.pbi.2013.02.005.

Li, C., Dong, N., Zhao, Y., Wu, S., Liu, Z., Zhai, J., 2021. A review for the breeding of orchids: current achievements and prospects. Hortic. Plant J. 7, 380–392. https://doi.org/10.1016/j.hpj.2021.02.006.

Li, Xiangjun, Yang, Y., Yao, J., Chen, G., Li, Xianghua, Zhang, Q., Wu, C., 2009. FLEXIBLE CULM 1 encoding a cinnamyl-alcohol dehydrogenase controls culm mechanical strength in rice. Plant Mol. Biol. 69, 685–697. https://doi.org/10.1007/s11103-008-9448-8.

Li, Y., Liu, G., Li, J., You, Y., Zhao, H., Liang, H., Mao, P., 2015. Acid detergent lignin, lodging resistance index, and expression of the caffeic acid O-methyltransferase gene in brown midrib-12 sudangrass. Breed. Sci. 65, 291–297. https://doi.org/10.1270/jsbbs.65.291.

Lopez, T., Runkle, E., Wang, Y.-T., Blanchard, M., Hsu, T., 2007. Growing the best phalaenopsis. Orchid 182–187.

Lv, G., Tang, D., Chen, F., Sun, Y., Fang, W., Guan, Z., Liu, Z., Chen, S., 2011. The anatomy and physiology of spray cut chrysanthemum pedicels, and expression of a caffeic acid 3-O-methyltransferase homologue. Postharvest Biol. Technol. 60, 244–250. https://doi.org/10.1016/j.postharvbio.2011.01.004.

McWhirter, K.S., 1979. Breeding of Cross Pollinated Crops. Plant breeding Aust Vice Cons Committee, Brisbane.

Meyer, N., 2010. Comparaison de variantes de régressionslogistiques PLS et de régression PLS sur variablesqualitatives : application aux donnéesd'allélotypage. J. Soc. Fr. Stat. 151, 1–18.

Milatović, D., Nikolić, D., Đurović, D., 2010. Variability, heritability and correlations of some factors affecting productivity in peach. Hort. Sci. (Prague) 37, 79–87. https://doi.org/10.17221/63/2009-HORTSCI.

Pagel, M., 1994. Detecting correlated evolution on phylogenies: a general method for the comparative analysis of discrete characters. Proc. R. Soc. B Biol. Sci. 255, 37–45. https://doi.org/10.1098/rspb.1994.0006.

Pagel, M., 1999. The Maximum Likelihood approach to reconstructing ancestral character states of discrete characters on phylogenies. Syst. Biol. 48, 612–622. https://doi.org/10.1080/106351599260184.

Pagel, M., Meade, A., 2006. Bayesian analysis of correlated evolution of discrete characters by reversible-jump Markov chain Monte Carlo. Am. Nat. 167, 808–825. https://doi.org/10.1086/503444.

Pagel, M., Meade, A., Barker, D., 2004. Bayesian estimation of ancestral character states on phylogenies. Syst. Biol. 53, 673–684. https://doi.org/10.1080/10635150490522232.

Paradis, E., Claude, J., Strimmer, K., 2004. APE: analyses of phylogenetics and evolution in R language. Bioinformatics 20, 289–290. https://doi.org/10.1093/bioinformatics/btg412.

Paradiso, R., De Pascale, S., 2014. Effects of plant size, temperature, and light intensity on flowering of Phalaenopsis hybrids in Mediterranean greenhouses. Sci. World J. 2014, 420807 https://doi.org/10.1155/2014/420807.

Pridgeon, A.M., Cribb, P.J., Chase, M.W., Rasmussen, F.N., 2014. Genera orchidacearum. In: Epidendroideae (Part 3), 6. Oxford University Press, Oxford, UK.

Pridgeon, A.M., Stern, W.L., Benzing, D.H., 1983. Tilosomes in roots of orchidaceae: morphology and systematic occurrence. Am. J. Bot. 70, 1365. https://doi.org/10.2307/2443427.

R Team, 2016. R: A language and Environment for Statistical Computing. R Foundation for Statistical Computing, Vienna, Austria.

R Team, 2019. RStudio: integrated development for R.

Rambaut, A., 2006. FigTree, Version 1.4.3. http://tree.bio.ed.ac.uk/software/figtree/.

Regmi, S., Poudel, B., Ojha, B.R., Kharel, R., Joshi, P., Khanal, S., Kandel, B.P., 2021. Estimation of genetic parameters of different wheat genotype traits in Chitwan, Nepal. Int. J. Agron. 2021, 1–10. https://doi.org/10.1155/2021/6651325.

Rencoret, J., Marques, G., Gutiérrez, A., Ibarra, D., Li, J., Gellerstedt, G., Santos, J.I., Jiménez-Barbero, J., Martínez, Á.T., del Río, J.C., 2008. Structural characterization of milled wood lignins from different eucalypt species. Holzforschung 62. https://doi.org/10.1515/HF.2008.096.

Revell, L.J., 2012. phytools: an R package for phylogenetic comparative biology (and other things). Ecol. Evol. 3, 217–223.

Roychowdhury, R., Randrianotahina, J., 2011. Evaluation of genetic parameters for agro-metrical characters in carnation genotypes. Afr. Crop Sci. J. 19, 183–188.

RStudio Team, 2020. RStudio: Integrated Development for R. RStudio, PBC, Boston, MA.

Rueden, C.T., Schindelin, J., Hiner, M.C., DeZonia, B.E., Walter, A.E., Arena, E.T., Eliceiri, K.W., 2017. ImageJ2: imageJ for the next generation of scientific image data. BMC Bioinform. 18, 529. https://doi.org/10.1186/s12859-017-1934-z.

Saroj, R., Soumya, S.L., Singh, S., Sankar, S.M., Chaudhary, R., Yashpal, Saini, N., Vasudev, S., Yadava, D.K., 2021. Unraveling the relationship between seed yield and yield-related traits in a diversity panel of *Brassica juncea* using multi-traits mixed model. Front. Plant Sci. 12, 651936 https://doi.org/10.3389/fpls.2021.651936.

Schindelin, J., Arganda-Carreras, I., Frise, E., Kaynig, V., Longair, M., Pietzsch, T., Preibisch, S., Rueden, C., Saalfeld, S., Schmid, B., Tinevez, J.Y., White, D.J., Hartenstein, V., Eliceiri, K., Tomancak, P., Cardona, A., 2012. Fiji: an open-source platform for biological-image analysis. Nat. Methods 9, 676–682. https://doi.org/10.1038/nmeth.2019.

Schoch, C.L., Sung, G.-.H., López-Giráldez, F., Townsend, J.P., Miadlikowska, J., Hofstetter, V., Robbertse, B., Matheny, P.B., Kauff, F., Wang, Z., Gueidan, C., Andrie, R.M., Trippe, K., Ciufetti, L.M., Wynns, A., Fraker, E., Hodkinson, B.P., Bonito, G., Groenewald, J.Z., Arzanlou, M., de Hoog, G.S., Crous, P.W., Hewitt, D., Pfister, D.H., Peterson, K., Gryzenhout, M., Wingfield, M.J., Aptroot, A., Suh, S.-.O., Blackwell, M., Hillis, D.M., Griffith, G.W., Castlebury, L.A., Rossman, A.Y., Lumbsch, H.T., Lücking, R., Büdel, B., Rauhut, A., Diederich, P., Ertz, D., Geiser, D. M., Hosaka, K., Inderbitzin, P., Kohlmeyer, J., Volkmann-Kohlmeyer, B., Mostert, L., O'Donnell, K., Sipman, H., Rogers, J.D., Shoemaker, R.A., Sugiyama, J., Summerbell, R.C., Untereiner, W., Johnston, P.R., Stenroos, S., Zuccaro, A., Dyer, P. S., Crittenden, P.D., Cole, M.S., Hansen, K., Trappe, J.M., Yahr, R., Lutzoni, F., Spatafora, J.W., 2009. The Ascomycota tree of life: a phylum-wide phylogeny clarifies the origin and evolution of fundamental reproductive and ecological traits. Syst. Biol. 58, 224–239. https://doi.org/10.1093/sysbio/syp020.

Schwallier, R., Gravendeel, B., de Boer, H., Nylinder, S., van Heuven, B.J., Sieder, A., Sumail, S., van Vugt, R., Lens, F., 2017. Evolution of wood anatomical characters in Nepenthes and close relatives of Caryophyllales. Ann. Bot. 119, 1179–1193. https://doi.org/10.1093/aob/mcx010.

Schweingruber, F.H., Börner, A., 2018. The Plant stem: A microscopic Aspect. Springer International Publishing, Cham. https://doi.org/10.1007/978-3-319-73524-5.

Serrano, A.M., Arana, M.V., Vanhaelewyn, L., Ballaré, C.L., Van Der Straeten, D., Vandenbussche, F., 2018. Following the star: inflorescence heliotropism. Environ. Exp. Bot. 147, 75–85. https://doi.org/10.1016/j.envexpbot.2017.11.007.

Sreeja, R., Balaji, S., Arul, L., Nirmala Kumari, A., Kannan Bapu, J.R., Subramanian, A., 2016. Association of lignin and FLEXIBLE CULM 1 (FC1) ortholog in imparting culm strength and lodging resistance in kodo millet (Paspalum scrobiculatum L.). Mol. Breed. 36, 149. https://doi.org/10.1007/s11032-016-0577-5.

Tang, C.Y., Chen, W.H., 2007. Breeding and development of new varieties in *Phalaenopsis*. Orchid Biotechnol. 1–22. https://doi.org/10.1142/9789812775900_0001. World Scientific.

Thonglim, A., Delzon, S., Larter, M., Karami, O., Rahimi, A., Offringa, R., Keurentjes, J.J. B., Balazadeh, S., Smets, E., Lens, F., 2020. Intervessel pit membrane thickness best explains variation in embolism resistance amongst stems of *Arabidopsis thaliana* accessions. Ann. Bot. https://doi.org/10.1093/aob/mcaa196.

Ullah, M.Z., Hasan, M.J., Chowdhury, A., Saki, A.I., Rahman, A., 2012. Genetic variability and correlation in exotic cucumber (*Cucumis sativus* L.) varieties. Bangladesh J. Plant Breed. Genet 25, 17–23.

Wani, M.R., Kozgar, M.I., Tomlekova, N., Khan, S., Kazi, A.G., Sheikh, S.A., Ahmad, P., 2014. Mutation breeding: a novel technique for genetic improvement of pulse crops particularly chickpea (*Cicer arietinum* L.). In: Ahmad, P., Wani, M.R., Azooz, M.M., Phan Tran, L.S. (Eds.), Improvement of Crops in the Era of Climatic Changes. Springer, New York, New York, NY, pp. 217–248. https://doi.org/10.1007/978-1-4614-8824-8_9.

Wickham, H., 2016. Ggplot2: Elegant Graphics for Data Analysis, 2nd Ed. Springer International Publishing.

Wyatt, R., 1982. Inflorescence architecture: how flower number, arrangement, and phenology affect pollination and fruit-set. Am. J. Bot. 69, 585–594. https://doi.org/10.1002/j.1537-2197.1982.tb13295.x.

Yadav, Y.C., Kumar, S., Bisen, B., Dixit, S.K., 2009. Genetic variability, heretability and genetic advance for some traits in cucumber. Indian J. Hortic. 66, 488–491.

Yang, Z., Kumar, S., Nei, M., 1995. A new method of inference of ancestral nucleotide and amino acid sequences. Genetics 141, 1641–1650. https://doi.org/10.1093/genetics/141.4.1641.

Yu, G., Smith, D.K., Zhu, H., Guan, Y., Lam, T.T.Y., 2016. GGTREE: an R package for visualization and annotation of phylogenetic trees with their covariates and other associated data. Methods Ecol. Evol. https://doi.org/10.1111/2041-210X.12628.

Zhao, D., Han, C., Tao, J., Wang, J., Hao, Z., Geng, Q., Du, B., 2012. Effects of inflorescence stem structure and cell wall components on the mechanical strength of

inflorescence stem in herbaceous peony. Int. J. Mol. Sci. 13, 4993–5009. https://doi.org/10.3390/ijms13044993.

Zhao, D., Luan, Y., Xia, X., Shi, W., Tang, Y., Tao, J., 2020. Lignin provides mechanical support to herbaceous peony (Paeonia lactiflora Pall.) stems. Hortic. Res. 7, 213. https://doi.org/10.1038/s41438-020-00451-5.

Zou, L.H., Huang, J.X., Zhang, G.Q., Liu, Z.J., Zhuang, X.Y., 2015. A molecular phylogeny of Aeridinae (Orchidaceae: epidendroideae) inferred from multiple nuclear and chloroplast regions. Mol. Phylogenet. Evol. 85, 247–254. https://doi.org/10.1016/j.ympev.2015.02.014.